

Dynamic Interfacial Tension Between a Thermotropic Liquid-Crystalline Polymer and a Flexible Polymer

Ruobing Yu,^{1,2} Wei Yu,² Chixing Zhou,² J. J. Feng^{3,4}

¹*School of Materials Science and Engineering 289, East China University of Science and Technology, Shanghai 200237, China*

²*Department of Polymer Science and Engineering, Shanghai Jiao Tong University, Shanghai 200240, China*

³*Department of Chemical and Biological Engineering, University of British Columbia, Vancouver, BC V6T 1Z4, Canada*

⁴*Department of Mathematics, University of British Columbia, Vancouver, BC V6T 1Z4, Canada*

Received 27 October 2005; accepted 5 January 2006

DOI 10.1002/app.24240

Published online in Wiley InterScience (www.interscience.wiley.com).

ABSTRACT: When a short fiber of a thermotropic liquid-crystalline polymer retracts in a quiescent, flexible polymer matrix, the polydomain texture inside the fiber evolves simultaneously. We have demonstrated experimentally that the two processes are coupled. The dynamic interfacial tension, determined from the retraction of the short fiber, decreases with time. On the other hand, we have determined the aspect ratio of the polydomains inside the fiber through the power spectra of two-dimensional discrete Fourier transformations of polarized optical microscopy images. The polydomains are initially elongated and aligned with the

fiber axis. As the fiber retracts into a spherical drop, the polydomains first retract into a circular shape and then are squeezed into elongated shapes perpendicular to the original fiber axis. An exponential function correlates the evolution of the dynamic interfacial tension with that of the aspect ratio of the textures. © 2006 Wiley Periodicals, Inc. *J Appl Polym Sci* 101: 3114–3120, 2006

Key words: thermotropic liquid-crystalline polymer (TLCP); interface; tension; aspect ratio

INTRODUCTION

In the past decades, many efforts have been made to understand the factors governing the morphology of immiscible blends.^{1–4} Interfacial tension is perhaps the most important factor, whose effects have been explored in drop deformation,^{5,6} breakup, and other relaxation processes. Zkik et al.⁷ showed nice illustrations of various effects induced by interfacial tension. Moreover, some methods, based on drop deformation or retraction, that are used to determine the interfacial tension can give reliable results for Newtonian fluids.^{8,9} The interfacial tension between two Newtonian fluids is a constant.¹⁰

Most previous investigations have focused on rheologically simple fluids, that is, Newtonian fluids. Recent experimental¹¹ and theoretical¹² studies have shown that the retractions of drops are highly dependent on the interfacial tension and viscoelasticity of

the component polymers. For simplicity, the effect of the viscoelasticity of component polymers can be integrated into the apparent interfacial tension, which can be regarded as the only driving force of drop retraction. The great influence of the shear history on the relaxation behavior of viscoelastic drops means that the apparent interfacial tension will be dependent on the extent of stretching of the macromolecules. Obviously, the usual concept for Newtonian polymers in determining the interfacial tension is not suitable for viscoelastic systems. An exception is when the macromolecules relax rapidly after the breakup of a thread, so the components behave as Newtonian fluids in the subsequent retraction of drops.¹⁰ However, if the relaxation time of the macromolecules is longer than the breakup time of the long fiber, the relaxation effect of the macromolecules should be considered in the drop retraction. Such a problem becomes even more complex if one fluid has internal anisotropic textures, as a thermotropic liquid-crystalline polymer (TLCP) does.

Experimental investigations of the interfacial tension between a TLCP and a flexible polymer are very limited. Machiels et al.¹³ measured the interfacial tension between a TLCP (Vectra A900) and a flexible polymer [poly(ether sulfone)] by the thread breakup method (TBM) and the fiber-retraction method (FRM). The TBM, based on Tomotika's theory¹⁴ for a pure Newtonian

Correspondence to: C. Zhou (cxzhou@sjtu.edu.cn).

Contract grant sponsor: National Natural Science Foundation of China; contract grant numbers: 20174024, 20204007, and 50290090.

Contract grant sponsor: U.S. National Science Foundation; contract grant numbers: CTS-9984402 and CTS-0229298.

system, requires a regular sinusoidal disturbance that grows in time. However, this has hardly ever been observed in a viscoelastic system, as shown in the experiments of Machiels et al. The FRM was suggested by Tjahjadi et al.¹⁵ and is based on the temporal evolution of the fiber shape during retraction. Wu and Mather¹⁶ measured the average interfacial tension between other TLCPs poly[(phenylsulfonyl)-p-phenylene 1,6-hexamethylenebis-(4-oxybenzoate)] and poly[(phenylsulfonyl)-p-phenylene 1,12-dodecamethylenebis(4-oxybenzoate)] and polydimethylsiloxane by the retraction of an ellipsoidal drop at different temperatures.

Generally, the relaxation time of a TLCP is much longer than that of a flexible-chain polymer. These long relaxation modes are ascribed to the complex polydomain structure of a TLCP. If the microstructures of a TLCP are not fully relaxed before the measurement of the interfacial tension by TBM or FRM, the orientation and deformation of the polydomains will vary with the shape relaxation of a TLCP drop or thread. This will cause the dynamic interfacial tension between a TLCP and a flexible-chain polymer to change with time during the measurements. The orientations of polydomains usually relax very quickly¹⁷ and can be ignored in the experiments of TBM or FRM. On the other hand, the relaxation of the aspect ratio of polydomains is a relatively slow process and should be considered for such measurements. Texture coarsening due to the coalescence of polydomains is still a much slower process and is not important for the measurement. Therefore, we believe that the most important process in TBM or FRM is the relaxation of the shape or aspect ratio of the polydomains. The results of Machiels et al.¹³ and Wu and Mather¹⁶ gave a constant apparent interfacial tension. Both involved only mild initial deformation of the TLCP polydomains, which would have been relaxed before the interfacial tension was measured.

A recent experiment by our group explored the influence of the deformation of polydomains on the interfacial tension and produced a time-dependent apparent interfacial tension.¹⁸ The method is the same as the one described by Mo et al.¹⁰ However, the semilog plot of the shape parameter $L^2 - B^2$ (L and B are half of the length and width of a drop, respectively) or the deformation parameter D [$D = (L - B)/(L + B)$] with time t is no longer a straight line when the drop phase is a TLCP. Then, the interfacial tension at time t is estimated from the local slope of the retraction curve by the theory of drop or fiber retraction. The interfacial tension thus obtained is an apparent value, whose variation with time can be ascribed to the change of the internal structures of the components. Here we refer to such an apparent interfacial tension changing with internal structure as dynamic interfacial tension.

These previous measurements suggest that, for polymer/TLCP blends, the dynamic interfacial tension depends greatly on the deformation of TLCP polydomains during drop or fiber retraction. However, little is known of the specifics of this dependence. In this article, we try to establish this relationship by a series of experiments on the retraction of short fibers with different initial stretch ratios.

EXPERIMENTAL

Materials

The materials used in this work were LC-5000 (Unichika, Inoue, Japan) and polycarbonate (PC; Makrolon 3103, Bayer, Leverkusen, Germany). LC-5000 exhibited a nominal melting point at 275°C, as measured with differential scanning calorimetry from the first heating scan with a heating rate of 20°C/min. At 295°C, LC-5000 becomes fully nematic. The glass-transition temperature of PC was 150°C.

As-received pellets of LC-5000 were dried at 180°C under nitrogen for 4 h and kept in vacuo at 90°C before further use. The matrix polymer, PC (Makrolon 3103), was dried and kept at 90°C in vacuo for at least 3 days before use.

All the rheological experiments were performed on a Gemini 200HR rheometer (Bohlin Instruments Co., Ltd., UK) with parallel plates with a diameter of 25 mm. The zero-shear viscosity of PC was determined by the fitting of the complex viscosity to the Ellis model and by the application of the Cox–Merz rule (viscosity of the matrix = 610 Pa s). Because LC-5000 did not show a plateau in the complex viscosity curve, it was difficult to determine its zero-shear viscosity from dynamic experiments. Therefore, creep tests under a small, constant stress (1 Pa) were performed to obtain the viscosity under a lower shear rate. The shear viscosity of LC-5000 was 115.1 Pa s. (The shear rate in the creep test was ca. 0.01 s⁻¹, in comparison with an estimated maximum strain rate of 0.014 s⁻¹ for fiber retraction. The shear rate obtained by the creep test was close to the shear rate during the fiber-retraction process. We can regard the shear viscosity obtained from the creep test as the shear viscosity of the dispersion.) The viscosity ratio between LC-5000 and PC was 0.189.

First, the LC-5000 melt was extruded from a capillary rheometer (RH7, Bohlin Instruments) at 295°C, and the extrudate was drawn from the die by a take-up device at drawing speeds of 400, 300, and 200 m/min. The polydomains of LC-5000 were stretched to different extents at different drawing speeds. As a result, various threads with different radii and stretch ratios were obtained. Then, the threads were cut into short fibers that were sandwiched between two PC matrix plates. The sandwich was molded into films

with a thickness of about 0.6 mm at 240°C. During the molding of the film, we increased the pressure gradually to drive out the air bubbles trapped around the TLCP fibers. Then, the film was cut into 8 mm × 8 mm squares, each containing one short fiber.

Observations were carried out on a polarized optical microscope (Leica, Wetzlar, Germany) with a camera and a hot stage at a magnification of 200×. The prepared specimen was put on the hot stage of the optical microscope and heated at 20°C/min to 240°C. The sample was maintained under this temperature for 5 min to allow the matrix polymer, PC, to relax completely. Therefore, only the variation of the texture of LC-5000 could possibly influence the interfacial tension. Subsequently, the specimen was heated further at 40°C/min to the desired temperature of 295°C. Then, the retraction of the short fiber was imaged and recorded. In most of our experiment systems, short fibers retracted to spheres, as shown in Figure 1. Image analysis software (Scion Image, Meyer Instruments, Inc., Houston, TX) was used to measure the change of the radius of a fiber with time and perform the two-dimensional discrete Fourier transform of the images inside a TLCP drop (discussed later).

Embedded FRM

During the retraction of a short fiber, its shape is not a standard ellipsoid (Fig. 1). Therefore, the accurate ellipsoidal model by Yu et al.⁸ cannot be used here to calculate the interfacial tension. Instead, we used the model of Carriere et al.¹⁹ for the retraction of a short fiber, which allows complex intermediate shapes such as dumbbells. This method has been successfully applied to the many systems, such as polystyrene/poly(methyl methacrylate),¹⁹ PC/polyethylene,²⁰ and polyamide 6/polystyrene.⁹

The short FRM¹⁹ involves microscopic tracking of the shape evolution of a short fiber embedded in a matrix. The interfacial tension is calculated from the characteristic relaxation time (τ) for retraction:

$$\tau = \frac{\eta_m + 1.7\eta_d}{2.7} \frac{R_e}{\sigma} \quad (1)$$

where η_m and η_d are the viscosities of the matrix and fiber, respectively. σ is the apparent interfacial tension. R_e is the radius of the final spherical drop. τ can be extracted from the following expression:

$$f(x) - f(x_0) = \frac{t}{\tau} \quad (2)$$

where

$$f(x) = \frac{3}{2} \ln \left(\frac{\sqrt{1+x+x^2}}{1-x} \right) + \frac{3\sqrt{3}}{2} \tan^{-1} \left(\frac{\sqrt{3x}}{2+x} \right) - \frac{x}{2} - \frac{4}{x^2} \quad (3)$$

where x is R/R_e and x_0 is R_0/R_e . R is the radius of the hemisphere at two ends of the short fiber, and R_0 is its initial value at $t = 0$ (the details of the model can be found in ref. 19).

The model of Carriere et al.¹⁹ for the retraction of a short fiber, in strict terms, is not a rigorous theory. However, its successful applications in the determination of the interfacial tension in Newtonian systems has proved it to be a good approximation of the retraction process of a short fiber.

Characterization of the polydomain structure inside the LC-5000 fiber

Light scattering (LS) methods are good choices for determining the deformation of the bulk texture of a TLCP.^{21,22} However, as light is very difficult to focus on a separate, small drop, it was difficult to apply LS methods here to detect the deformation of polydomains inside a TLCP drop. Instead, we use polarized optical microscopy (POM). The aspect ratio of the deformed texture was obtained from the power spectrum of two-dimensional discrete Fourier transformations (DFTs) of the image inside a TLCP drop. Although the DFT of POM is not as sensitive as LS,²² it serves very well our purpose of correlating the dynamic interfacial tension with the shape and deformation of TLCP polydomains.

RESULTS

A typical retracting process is shown in Figure 1 for a short TLCP fiber (drawn at a speed of 300 m/min) in a PC matrix. The fiber retracts into a spherical shape after about 134 s. During the retraction process, the texture inside the TLCP fiber changes significantly. This is completely different from the drop-retraction process in flexible-chain polymer systems.^{9,10} Initially, the short fiber shows a strong orientation of textures along the long axis of the fiber ($t = 0$). Such orientation order is due to the fast drawing process after capillary extrusion. Driven by interfacial tension, the TLCP short fiber retracts into a dumbbell-like shape, then an ellipsoid, and finally a sphere. In the meanwhile, the initially strong orientation of the texture along the fiber gradually disappears, giving way to an orientation perpendicular to the long axis of the fiber. The variation of the texture is due to the flow field inside the fiber. According to simulations on drop retraction,²³ flow appears perpendicular to the long axis of the drop (see Fig. 2). Mather et al.²⁴ found that, for

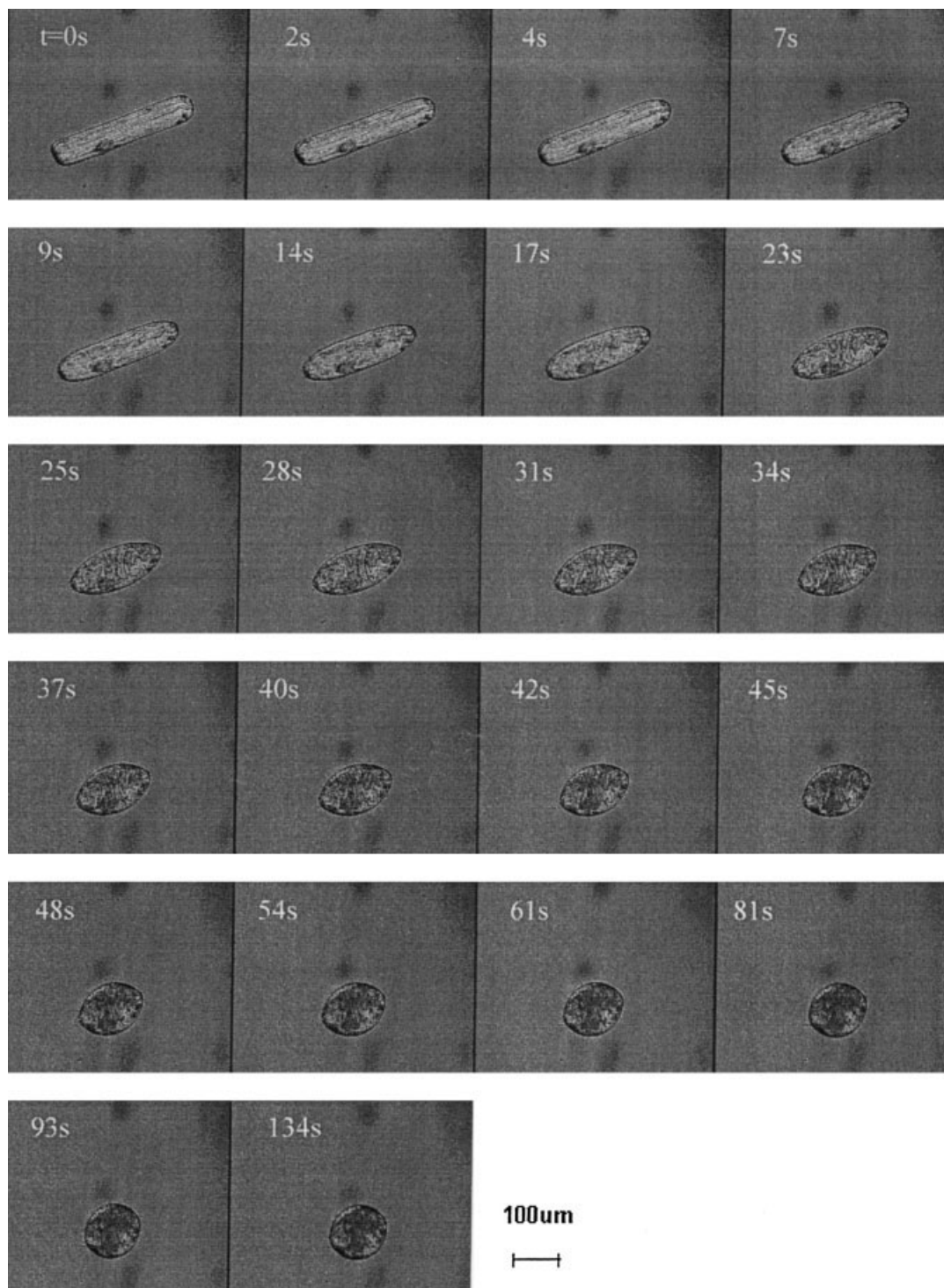


Figure 1 Retraction of an LC-5000 short fiber drawn at a speed of 300 m/min at 295°C.

lyotropic LCP, the application of a second shear in the orthogonal direction resulted in the formation of bands orientated perpendicularly to the original shear direction but parallel to the second shear direction. Therefore, the orientation of TLCP perpendicular to the long axis of the fiber is due to the appearance of flow in this direction inside the fiber during the retraction process.

The apparent interfacial tension is calculated from the Carriere–Cohen–Arends model. A typical plot of $f(x) - f(x_0)$ versus time t of a TLCP short fiber embedded in a PC matrix is shown in Figure 3. As the Carriere–Cohen–Arends model is derived for Newtonian systems, it is not surprising that it fails to fit the data with a constant interfacial tension. However, the model can be used locally to produce a time-depen-

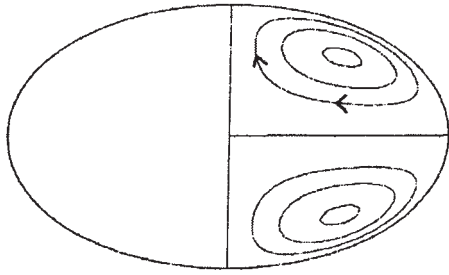


Figure 2 Streamline inside the drop during drop retraction.

dent dynamic interfacial tension.¹⁸ This apparent interfacial tension represents the overall effect of the anisotropic interface between the TLCP and the flexible-chain matrix. Figure 4 shows that for fibers produced at three drawing speeds, the dynamic interfacial tension decreases with time, from about 8–10 to about 1–2 mN/m. Somewhat surprisingly, the drawing speed does not seem to have a consistent effect. We will return to this point later.

To correlate the dynamic interfacial tension with the evolution of the texture inside the TLCP fiber, we use two-dimensional DFTs of the images inside an LC-5000 fiber. Representative power spectra are shown in Figure 5. Although it is difficult to determine quantitatively the deformation of textures from images of POM, the power spectrum shows an ellipsoidal shape, which can be correlated with the polydomain geometry in real space. A schematic illustration of this correlation is shown in Figure 6; an ellipsoidal domain inside the TLCP fiber gives rise to an ellipsoidal pattern in the power spectrum with the same aspect ratio but rotated by 90°. The aspect ratio of the polydomain (b/a) is the average of many domains. The evolution of b/a during retraction is shown in Figure 7, where a

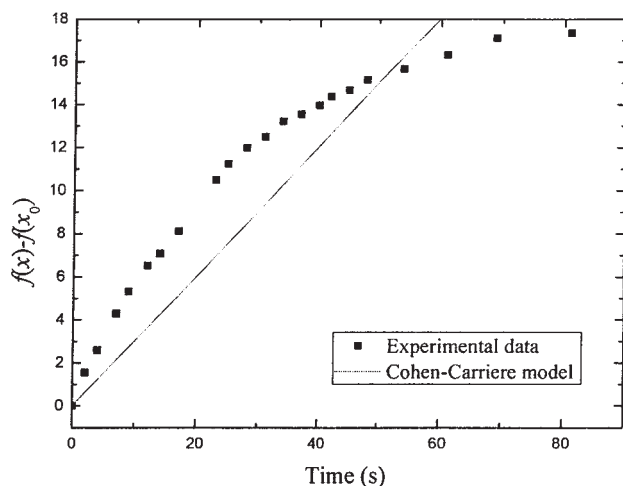


Figure 3 Typical plot of $f(x) - f(x_0)$ versus retraction time t for an LC-5000 fiber embedded in a PC matrix (for a fiber at a drawing speed of 300 m/min at 295°C).

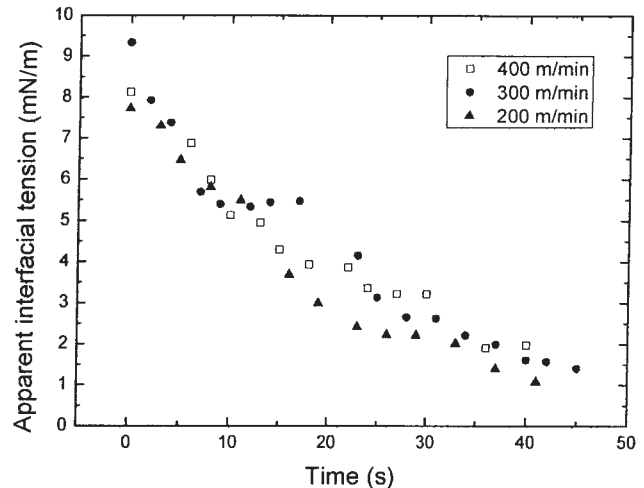


Figure 4 Time evolution of the dynamic interfacial tension between LC-5000 and PC.

and b are the axis lengths of the stretched polydomain parallel and perpendicular to the long axis of the short fiber, respectively. b/a increases from about 0.7–0.8 to 1.3–1.4 during drop retraction. This means that the initially elongated polydomains along the long axis of the fiber relax first to an intermediate state that is roughly circular ($b/a = 1$) and then stretch along the direction perpendicular to the long axis of the fiber, evidently being squeezed by the flow due to drop retraction. The influence of the texture evolution on the retraction of a TLCP fiber is reflected in the dynamic interfacial tension, which shows a fast decrease within the first 25 s of retraction and a much slower decrease after that (Fig. 4). This transition time is consistent with the relaxation of deformed TLCP polydomains changing from being parallel to the fiber to being perpendicular to the fiber. Therefore, we suggest that the decrease of the dynamic interfacial tension with time is due to the relaxation of deformed polydomains. We remind the reader that σ in Figure 4, calculated from fiber retraction, represents an apparent interfacial property. It depends strongly on the TLCP texture inside the drop.

Two additional remarks should be made here. First, the aspect ratio of polydomains does not relax to 1 after a TLCP fiber retracts to a sphere. This is probably due to the fact that the relaxation time of deformed polydomains is longer than the retraction time of a fiber. Thus, the evolution in Figure 7 has much to do with convection and little to do with elastic relaxation. It is expected that the polydomain texture will relax eventually, on a timescale much longer than that of the fiber retraction. Second, the aspect ratios of polydomains inside a TLCP fiber do not show much difference for fibers with different drawing speeds. In fact, higher drawing speeds do not seem to cause more elongated polydomains. We conjecture that a suffi-

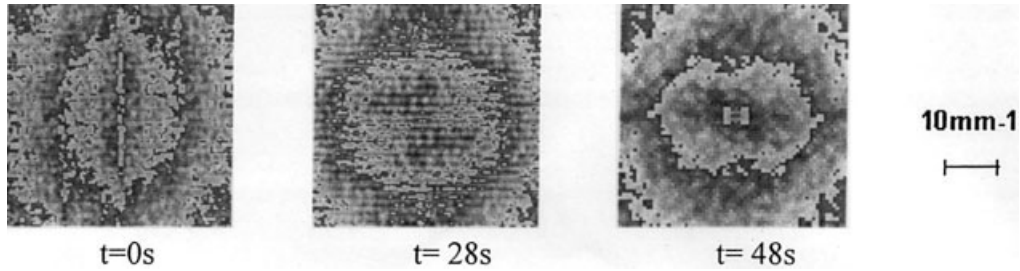


Figure 5 Typical power spectra of two-dimensional DFTs of the images in Figure 1.

ciently high drawing speed will break up polydomains into smaller one, with a final aspect ratio that does not depend greatly on the applied drawing speed. The drawing speeds in our experiments are believed to be large enough to break up the polydomains.

We plot the dynamic interfacial tension against b/a in Figure 8. The dynamic interfacial tension decreases with an increase in the aspect ratio. This can perhaps be understood by the visualization of the following scenario. Initially, the polydomains are aligned with the fiber, and their retraction assists the retraction of the fiber. Hence, the large apparent interfacial tension appears. In contrast, the later squeezing of the polydomains into transverse strips tends to hamper the retraction of the fiber and produce a smaller apparent interfacial tension. The following exponential function fits the data for all three fibers drawn at different speeds:

$$\frac{\sigma - \sigma_{\min}}{\sigma_e - \sigma_{\min}} = ke^{-\frac{b/a-1}{\beta}} \quad (4)$$

The fitting parameters are $\sigma_{\min} = 0.078$ mN/m, $\sigma_e = 3.69$ mN/m, $k = 0.960$, and $\beta = 0.304$. σ_{\min} is a minimum dynamic interfacial tension that corresponds to polydomains with infinite b/a oriented perpendicularly to the original long axis of the TLCP fiber. σ_e is

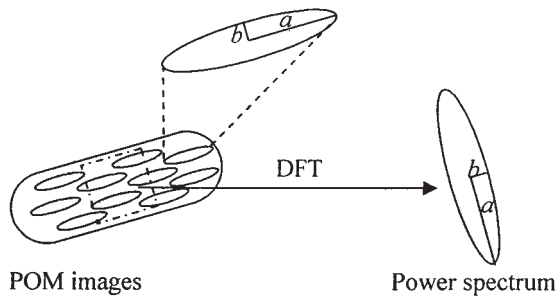


Figure 6 Schematic of the polydomains inside a TLCP short fiber and its power spectrum. b and a represent the lengths of semi-axes of deformed polydomains perpendicular and parallel to the long axis of the fiber, respectively.

regarded as an equilibrium value approached when the textures are not deformed ($b/a = 1$). Equation (4) embodies the observations made earlier: the dynamic interfacial tension is larger than σ_e when the textures deform along the long axis of the fiber and smaller than σ_e when the textures deform perpendicularly to the long axis of the fiber.

CONCLUSIONS

The dynamic interfacial tension can be determined as a function of time by the application of the model of Carriere et al.¹⁹ to short fiber retraction. The aspect ratio of polydomains inside a TLCP fiber has been analyzed by the power spectra of two-dimensional DFTs of the POM image. The variation of the dynamic interfacial tension coincides with the deformation of the polydomains. An exponential function has been used to correlate the dynamic interfacial tension and the aspect ratio of the polydomains. The equilibrium interfacial tension corresponds to the undeformed texture (the aspect ratio is 1). The dynamic interfacial tension is larger than 3.69 mN/m if the polydomains deform along the long axis of a TLCP fiber and is

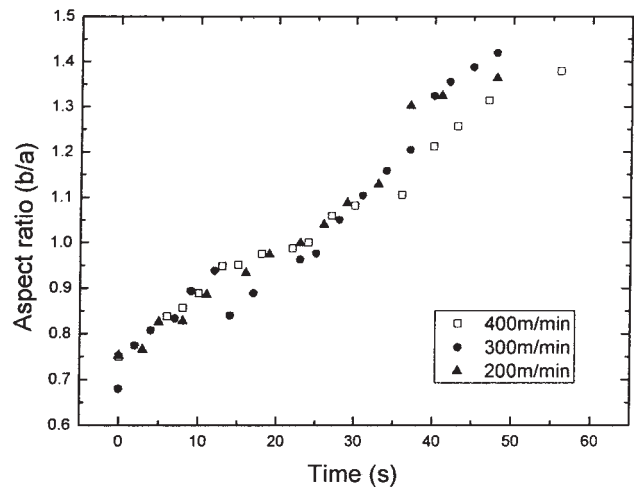


Figure 7 Evolution of b/a for a TLCP with time.

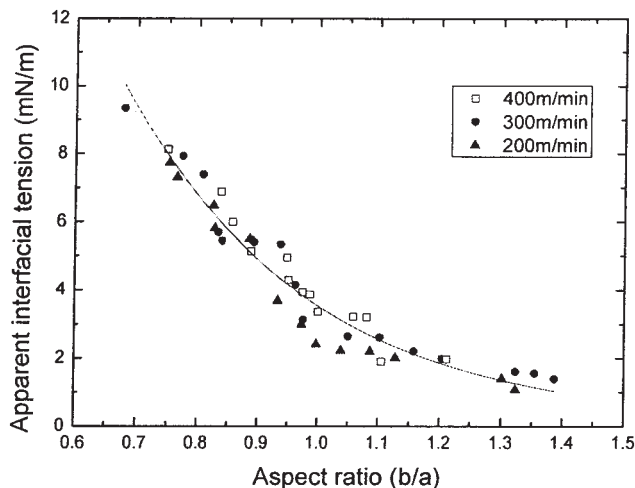


Figure 8 Dynamic interfacial tension between LC-5000 and PC versus b/a for LC-5000.

smaller than 3.69 mN/m if the polydomains deform perpendicularly to the long axis of a TLCP fiber.

References

- Rallison, J. M. *Annu Rev Fluid Mech* 1984, 16, 45.
- Tucker, C. L.; Moldenaers, P. *Annu Rev Fluid Mech* 2002, 34, 177.
- Yu, W.; Bousmina, M.; Grmela, M.; Paliarne, J. F.; Zhou, C. X. *J Rheol* 2002, 46, 1381.
- Yu, W.; Bousmina, M.; Grmela, M.; Paliarne, J. F.; Zhou, C. X. *J Rheol* 2002, 46, 1401.
- Jackson, N. E.; Tucker, C. L. *J Rheol* 2003, 47, 659.
- Yu, W.; Bousmina, M. *J Rheol* 2003, 47, 1011.
- Zkiek, A.; Yu, W.; Bousmina, M.; Grmela, M. *Rheol Acta* 2004, 43, 333.
- Yu, W.; Bousmina, M.; Zhou, C. X. *Rheol Acta* 2004, 43, 342.
- Xing, P.; Bousmina, M.; Rodigue, D.; Kamal, M. R. *Macromolecules* 2000, 33, 8020.
- Mo, H. Y.; Zhou, C. X.; Yu, W. *J Non-Newtonian Fluid Mech* 2000, 91, 221.
- Tretheway, D. C.; Leal, L. G. *J Non-Newtonian Fluid Mech* 2001, 99, 81.
- Yu, W.; Bousmina, M.; Zhou, C. X.; Tucker, C. L. *J Rheol* 2004, 48, 417.
- Machiels, A. G. C.; Busser, R. J.; Van Dam, J.; Posthuma De Boer, A. *Polym Eng Sci* 1998, 38, 1536.
- Tomokita, S. *Proc R Soc London Ser A* 1935, 150, 322.
- Tjahjadi, M.; Ottino, J. M.; Stone, H. A. *AIChE J* 1994, 40, 385.
- Wu, J.; Mather, P. T. *Proc Annu Meet Soc Rheol* 2002, 10, HS12.
- Wiberg, G.; Hillborg, H.; Gedde, U. W. *Polym Eng Sci* 1998, 38, 1278.
- Yu, R. B.; Yu, W.; Zhou, C. X.; Feng, J. J. *J Appl Polym Sci* 2004, 94, 1404.
- Carriere, C. J.; Cohen, A.; Arends, C. B. *J Rheol* 1989, 33, 681.
- Pham, H. T.; Carriere, C. J. *Polym Eng Sci* 1997, 37, 636.
- Ernst, B.; Navard, P. *Macromolecules* 1989, 22, 1419.
- Hsiao, B. S.; Stein, R. S.; Deutscher, K.; Winter, H. H. *J Polym Sci Part B: Polym Phys* 1990, 28, 1571.
- Hooper, R. W.; De Almeida, V. F.; Macosko, C. W.; Derby, J. J. *J Non-Newtonian Fluid Mech* 2001, 98, 141.
- Mather, P. T.; Jeon, H. G.; Han, C. D.; Chang, S. *Macromolecules* 2000, 33, 7594.